Bulk CO_2-based Amorphous Triols Used for Designing Biocompatible Shape-Memory Polyurethanes

Shunjie Liu[1,2], Yusheng Qin[*,1], Xianhong Wang[*,1] and Fosong Wang[1]

[1]*Key Laboratory of Polymer Ecomaterials, Changchun Institute of Applied Chemistry, Chinese Academy of Sciences, Changchun 130022, People's Republic of China*
[2]*University of Chinese Academy of Sciences, Beijing 100039, People's Republic of China*

Received December 12, 2014; Accepted March 11, 2015

ABSTRACT: Precursors with sharp crystalline transition temperature have attracted significant attention in the field of shape-memory materials; however, seldom have reports been related to amorphous ones with industrial application prospects. This study introduced a new family of amorphous CO_2-based hydroxyl-telechelic three-armed oligo(carbonate-ether) triol (Triol) with controllable molecular weight (M_n) and carbonate unit content (CU), which was coupled with PEG and 1,6-hexamethylene diisocyanate (HDI) to afford crosslinked polyurethanes (PU) networks with well-defined architecture. A crosslinking point was provided by Triol and PEG was used to afford networks some crystallinity. The resulting networks were characterized using attentuated total reflectance Fourier transform infrared spectroscopy (ATR-FTIR) and differential scanning calorimetry (DSC), and the shape-memory effect test provided insight into the relationship between shape memory behaviors and polymeric structures. The networks displayed good dual-shape memory effect when compared with others: shape fixity ratio (R_f) could be controlled by changing the Triol content and M_n, and all the shape recovery ratios (R_r) of the networks could unexpectedly approach 100% under the experimental conditions. Interestingly, the substructure of the Triol CU, could effectively regulate the recovery time of the networks, e.g., the recovery time decreased with the increment of Triol CU without changing R_f and R_r. Besides, crystalline transition temperature could be simply changed by altering Triol content. A typical sample Triol(2k, 50%)$_{40}$-PEG(6k)$_{60}$ displayed excellent dual-shape effect with almost 100% R_f and R_r at a recovery time of 40 s at 70°C. More interestingly, this sample could almost immediately recover its original shape (in less than 3 s) when immersed in 70°C water. Direct contact and MTT tests were used for assessment of cell viability and proliferation. These results confirmed the potential of these polyurethanes as a new family of tunable biomedical shape-memory materials.

KEYWORDS: Carbon dioxide, amorphous, polyol, shape-memory, polyurethane

1 INTRODUCTION

Shape-memory materials are a class of smart materials with the ability to change shape on command in response to an environmental stimulus. Although shape-memory alloys (SMAs) are currently the most prominent and widely used, they suffer from limited recoverable strains (< 8%), high cost, and a comparatively inflexible transition temperature [1]. Such limitations have provided motivation for the development of alternative materials, especially shape-momery polymers (SMPs). The SMPs possess many prominent characteristics such as highly flexible programming, broad range of structural designs, lower-cost processing and significantly larger recovery strain [2,3], and can be triggered by various stimuli such as heat [4,5], light [6,7], magnetic field [8], etc. Consequently, the merits mentioned above enable SMPs to be emerging materials for use in a variety of areas, such as intelligent biomedical devices [9], sensors and actuators [10], and heat-shrink tubing [11].

Thermally induced SMPs are one of the most widely studied SMPs as they can be easily obtained and programmed [1]. Furthermore, the most fascinating virtue of SMPs is that there is an abundance of approaches for designing net-points and switches for various types of SMPs [12]. Typically, thermally induced SMPs consist of two phases: one of them is a fixed phase and the other is a reversible or switching one [13]. The permanent shape is determined by chemical (covalent

*Corresponding authors: ysqin@ciac.ac.cn; xhwang@ciac.ac.cn

DOI: 10.7569/JRM.2014.634140

bonding) or physical (crystalline segregated domains or entanglements in ultra-high molecular weight polymers) crosslinks, and glass transition or melting of crystalline of molecular chains can be designed as a reversible phase for deformation from original shape to temporary shape. In general, thermal shape-memory testings are programmed by applying a constant force or a target strain to the polymer above a given transition temperature (T_{trans}), which can consist of a glass transition (T_g) or melting transition (T_m). The freeze of segment motion associated with T_g or the formation of crystalline domains associated with (T_m) under low temperature (< T_{trans}) lead to shape fixation. The shape-memory effect is then activated by reheating the sample above T_{trans} and is driven by crosslinks within the system via entropic elasticity [14,15]. Because different polymers exhibit different glass transition temperatures and melting temperatures, they can display shape memory effects in various temperatures, fulfilling variable requirements of practical applications.

Polyurethane-type SMPs are one of the most widely studied thermally induced SMPs that have drawn increasing attention since their discovery in 1988 [16,17]. Initially, most of the research concentrated on physically crosslinked segmented polyurethanes, due to the easier processibility. However, it is normally observed in physically crosslinked shape memory polyurethane systems that they are prone to creep and have some irreversible deformation during "memory programming" [18]. Much work has been done to overcome these drawbacks with variable success. In 1998, Kim *et al.* [19] prepared ionic polyurethanes by introducing acids to a crystalline polycaprolactone diols (PCL) 4,4'-diphenylmethane diisocyanate (MDI) system, which displayed higher recovery strain and lower residual strain compared with non-ionomers. However, cyclic hardening (resistance to deformation with cycling) was harmful to the shape-memory effect. In the same year, Chen *et al.* [18] developed high hard-segment content polyurethanes from low molecular weight polytetramethylene oxide glycol (PTMO) having good shape-memory effects. Nevertheless, creep still existed as the number of testings increased. Then polyurethanes with mesogenic moiety were synthesized from PCL-MDI system in the presence of mesogenic chain extenders, which improved the dissolution of the hard segment and therefore the shape fixity. However, the creep could still not be overlooked [20]. Therefore, chemically crosslinking as a method to resist creep has received much consideration in the synthesis of shape-memory polyurethanes. Early in 1999, Chen *et al.* [21] reported crosslinked PU by introducing trimethylol propane (TMP) into a crystalline poly(butylene adipate) glycol (PBAG)-MDI system. However, no crystalline domain was found in the DSC spectra, which was disturbed by crosslinked structure. In 2005, Lendlein *et al.* [22] reported the first biodegradable copolyester-urethane networks crosslinked by oligo[(rac-lactide)-glycolide] polyols. Besides excellent shape-memory effect, the transparent networks also showed a more homogeous degradation. In 2006, Shi *et al.* [23] developed a series of hybrid polyurethanes crosslinked by Si-O-Si domains, resulting in a fast shape recovery speed (less than 10 s in water at 25°C). The Si-O-Si linkages not only acted as the netpoints but also acted as inorganic fillers for reinforcement. More recently, Wang *et al.* [12] prepared dual-shape PU networks from crystalline three-armed poly(p-dioxanone) (PPDO)-PEG systems. Later, they developed a novel interpenetrating polymer network constructed by self-complementary quadruple hydrogen bonding and covalent bonding, which displayed excellent triple-shape memory effect as designed [24]. Bonfil *et al.* [25] prepared shape-memory polyurethanes by using castor oil (CO) as crosslinking points and PEG with different M_n as transition domain, which could tailor transition temperature close to body temperature. Nevertheless, it was not possible to prepare networks lower than 50:50 of CO:PEG ratio, and R_f and R_r could hardly reach 100%. As seen from the discussion above, the types of macromolecular crosslinking agents were limited, and more attention was focused on the crystalline but not amorphous ones. In addition, crosslinking agents with accurate M_n or having large industrial output were seldom reported. Consequently, there is an urgent need to explore new polyols on a large scale to stimulate the further development of SMPs.

Given the diversity in selection of crosslinking agents, amorphous CO_2-based hydroxyl-telechelic three-armed oligo(carbonate-ether) triol (Triol) can be used to construct thermoset polyurethanes with shape-memory properties. The Triols are low-molecular weight polyether carbonates copolymerized by CO_2 and propylene oxide in the presence of chain transfer agents, which are potential large-scale (in millions of ton) raw materials in the global modern polyurethane industry. Herein, a high-yield facile synthesis of Triol has been realized by our group [26]. Moreover, the M_n and CU of the Triols can be accurately adjusted to endow polyurethanes with new thermal and mechanical performances. Therefore, these Triols can substantially extend the spectrum of potential industrial applications for SMPs. PEG, an aliphatic polyether with good crystallinity, is suitable for use as transition domain to construct shape-memory polymers. In the present work, amorphous Triol was coupled with crystalline PEG to prepare shape-memory networks, where Triol was used as macromolecular crosslinking agent to determine the permanent shape, and PEG could be designed as reversible phase for deformation.

2 EXPERIMENTAL

2.1 Materials

Oligo(carbonate-ether) triol (Triol) was prepared following a literature procedure developed in this lab [26]. Other reagents with analytical purity were used as received.

2.2 Synthesis of Oligo(carbonate-ether) Triol-poly(ethylene glycol) (Triol-PEG) Networks

(Triol-PEG) networks with different contents were prepared according to the previously reported methods [12]. Firstly, PEG-diol and Triol were mixed in a reaction vessel and dried at 80°C under vacuum for 3 h to complete dehydration. Then the precursors were diluted with the Anhydrous N,N-dimethylformamide (DMF); a predetermined amount of HDI (the mole ratio of –NCO/-OH was 1.05:1) was injected to initiate the coupling reaction as soon as the reactants were completely dissolved. After 3 h at 80°C, the mixture was injected into a horizontal Teflon dish in a glass autoclave under the protection of a nitrogen stream. After 48 h of reaction, the networks were transferred into a drying oven for 2 days at 75°C and then dried under vacuum. All samples were recorded as Triol(a, c)$_m$-PEG(b)$_n$, where a and b represented the M_n of triol and PEG, respectively, c represented the CU of the triol, and the subscripts x and y were the weight fractions of Triol and PEG, respectively. The average functionality ($\bar{f}$) of the precursors was calculated based on the feed ratio of triol and PEG diol by the following formula:

$$\bar{f} = \frac{n_{Triol} \times 3 + n_{PEG} \times 2}{n_{Triol} + n_{PEG}}$$

2.3 Characterization

The FTIR spectra of the samples were recorded on a Bruker TENSOR-27 spectrophotometer using a ZnSe ATR crystal with spectral resolution of 2 cm^{-1}, where the molded blends' sheets were pressed directly onto the ZnSe crystal with a close contact. Differential scanning calorimetry (DSC) measurements were performed on a PerkinElmer DSC-7 instrument under a N_2 atmosphere. The samples were first heated from –50°C to 100°C at 10°C/min and then rapidly quenched to –50°C, followed by the second heating process in the same way as the first. The glass transition temperature (T_g) was defined as the value of midpoint of transition in the second heating process. The unit of ΔH was J/g, with g referring to the quality of the sample measured.

2.3.1 Mechanical test

Tensile tests were carried out using dumbbell-shaped samples punched out from the molded sheets. The test was performed by a screw-driven universal testing machine (Z010, Zwick Co., Germany) equipped with a 10 kN electronic load cell and mechanical grips. The tests were conducted at room temperature using a crosshead rate of 10 mm/min according to the ASTM standard, and the data reported were the mean of the parallel values in five determinations.

2.3.2 The swelling ratio and gel content of the triol-PEG network

Triol-PEG network samples were cut into small slices, swelled and extracted by methylene dichloride for 24 h. The mass of the unextracted sample (m_0), the swelled extracted sample (m_s) and the dried extracted sample (m_d) were recorded. The swelling ratio (S(%)) and gel content (G(%)) were calculated by the following formulas [12]:

$$S(\%) = \frac{m_s}{m_d} \times 100\%$$

$$G(\%) = \frac{m_d}{m_0} \times 100\%$$

All of these data were measured three times and averaged.

2.3.3 Shape-memory effect (SME)

The bending test method was adopted to evaluate the shape-memory properties. The specimens were cut into rectangular strips with the dimension of 60 mm×4 mm×1 mm. The test was carried out by the following procedures:

The program of the shape-memory property test was conducted as follows: firstly, the specimens (60 mm×4 mm×1 mm) were heated to T_m + 20°C and kept for 10 min before they were bent to a given angle θ_{max} (in the present work, θ_{max} = 149°); subsequently they were quenched to a low temperature T_{low} (room temperature) and kept for another 10 min in the bent condition. After that, the external force was released and the samples turned to an angle θ_{fixed}; finally, each specimen was heated to T_m + 20°C for 10 min. When the recovery ended, the angle θ_{final} was recorded. The shape fixity ratio (R_f) and shape recovery ratio (R_r) were calculated according to the following formulas [12]:

$$R_f = \frac{\theta_{fixed}}{\theta_{max}} \times 100\%$$

$$R_r = \frac{\theta_{fixed} - \theta_{final}}{\theta_{fixed}} \times 100\%$$

All of these data were measured three times and averaged.

2.3.4 *Cytotoxicity assay*

The Triol(2k, 50%)$_{60}$-PEG(6k)$_{40}$ was cut into four parts: 1 mg (0.75 mm × 6 mm), 2 mg (1.5 mm × 6 mm), 4 mg (3 mm × 6 mm), 8 mg (6 mm × 6 mm). Then they were sterilized for 30 min in 70% ethanol containing 150 U/mL antibiotics under UV light and then washed with PBS (phosphate buffered saline) twice. The viability and proliferation of Hela cells were evaluated by two methods: direct contact test and methyl thiazolyl tetrazolium (MTT) assay [25].

In direct contact test, Hela cells were incubated in the culture medium at 37°C in an atmosphere of 5% CO_2 and 95% air for 24 h. Subsequently, the culture medium was removed. The cells were incubated in culture medium containing Triol(2k, 50%)$_{60}$-PEG(6k)$_{40}$ networks with different contents for another 24 h. The morphological changes indicating cytotoxicity and cell growth characteristics were observed using an inverted microscope. Wells containing cells but no polymer were used as control.

In MTT assay, typically, Hela cells were incubated in the culture medium at 37°C in an atmosphere of 5% CO_2 and 95% air for 24 h. Subsequently, the culture medium was removed. The cells were incubated in culture medium containing Triol(2k, 50%)$_{60}$-PEG(6k)$_{40}$ networks with different contents for another 24 h and washed with medium twice. 100 μL of the new culture medium containing MTT reagent (10%) was added to each well of the 96-well assay plate and incubated for 4 h to allow formation of formazan dye. After removal of the medium, the purple formazan product was dissolved with DMSO for 15 min. Finally, the optical absorption of formazan at 570 nm was measured by an enzyme-linked immunosorbent assay reader. Wells containing cells but no polymer were used as control experiment to evaluate the effects of the polymers. Reported values are the mean of three replicates and are expressed as percentages of the control values.

3 RESULTS AND DISCUSSION

3.1 Preparation of Oligo(carbonate-ether) Triol with Different M_n and CU

Oligo(carbonate-ether) triol with controlled M_n and CU was prepared as depicted in Scheme 1. Table 1 lists the M_n and CU of Triol calculated by ^{1}H NMR.

3.2 Preparation of Triol-PEG Networks

Since high molecular weight PEG has relatively high crystallinity in combination with its chemical reactivity, the present work solely uses PEG (6k) as one of the precursors to prepare Triol-PEG networks. As is shown in Scheme 2, the networks were synthesized from star-shaped Triol and linear PEG diol in the presence of HDI. Table 2 displays the basic parameters (Triol content, S (%), G (%)) of the networks. The swelling ratio of the Triol-PEG networks increased with increasing Triol content and chain length of the Triol segment due to the lower crosslink density. Conversely, the gel content increased with the higher crosslink density. For example, S (%) of Triol-PEG network increased from 550% to 1350%, while G (%) decreased from 77% to 37%, as can be seen from entries 1-3, Table 2. The low gel content (< 80%) indicates that the structure of the network may be the mixture of networks and branched copolymers. The ATR-FTIR spectrum of Triol-PEG networks (Figure S1) confirms the formation of CO_2-based polyurethane networks.

3.3 Thermal Transition Behavior of Triol-PEG Networks

As we know, thermal transition behavior is very important to materials, especially to thermally induced shape-memory polymers, as it dominates

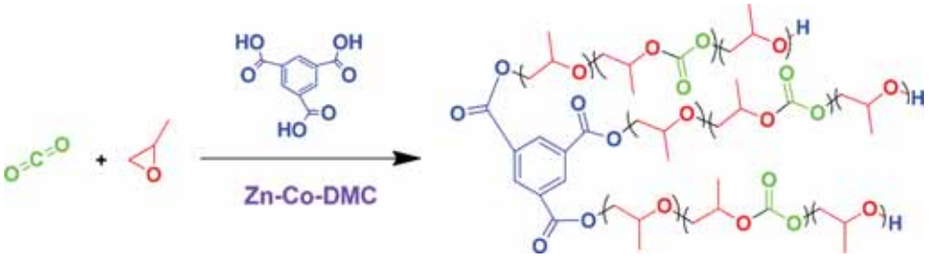

Scheme 1 Synthesis of oligo(carbonate-ether) triol.

Table 1 Preparation of Triol precursor.

Sample	M_n [a] (g mol^{-1})	CU[a] (%)	M_n [b] (g mol^{-1})	PDI[b]
Triol(2k)	1950	20	2600	1.11
Triol(2k)	1900	35	2400	1.17
Triol(2k)	1950	50	2600	1.23
Triol(1.5k)	1450	35	2000	1.18
Triol(4k)	3850	35	5100	1.45

a: Calculated by ^{1}H NMR according to Ref. [26],
where $M_n = 102[(A_{5.0}+A_{4.2}+3A_{5.2}-3*A_{8.8}-2A_{4.58})/A_{8.8}]$
$+58[(A_{3.5}+3A_{8.8}-2A_{5.2})/A_{8.8}]+210;$
$CU = (A_{5.0}+A_{4.2}+3A_{5.2}-2A_{4.58}-3A_{8.8})/(A_{5.0}+A_{4.2}+A_{5.2}+A_{3.5}-2A_{4.58}).$

b: Measured by GPC at 35°C, where polystyrene is used as standard, CH_2Cl_2 as eluent, and flow rate is set at 1.0 ml min^{-1}.

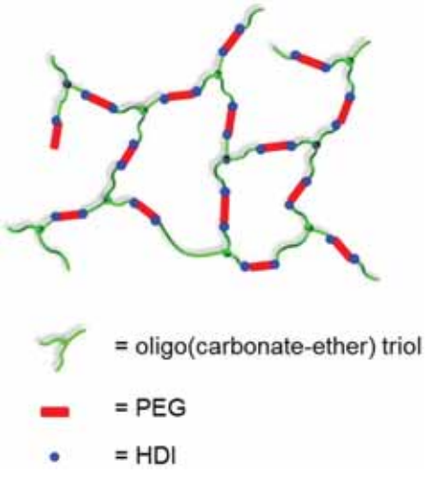

Scheme 2 Schematic diagram of the structure of the Triol-PEG networks.

the transition temperature, so as to affect the shape-memory performance of the networks. Thus, all the thermal properties and characteristic temperatures such as the glass transition temperature (T_g), recrystallizing temperature (T_c), and crystal melting temperature (T_m) of the networks were measured using DSC [18]. In the Triol-PEG networks, Triol was used as macromolecular crosslinking agent to determine the permanent shape of the networks; PEG could be designed as reversible phase for deformation, due to its strong crystalline ability. The crystallization behavior of the Triol-PEG network, the influence of the weight fraction, the carbonate unit content and molecular weight of Triol were explored by DSC detailedly.

Table 2 Basic parameters of Triol-PEG networks.

Entry	Samples	$\bar{f}^a$	S (%)	G (%)
1	Triol(2k, 50%)$_{40}$-PEG(6k)$_{60}$	2.67	1350	37
2	Triol(2k, 50%)$_{50}$-PEG(6k)$_{50}$	2.75	1000	53
3	Triol(2k, 50%)$_{60}$-PEG(6k)$_{40}$	2.81	550	77
4	Triol(2k, 20%)$_{40}$-PEG(6k)60	2.67	1150	32
5	Triol(2k, 20%)$_{60}$-PEG(6k)$_{40}$	2.81	570	78
6	Triol(2k, 35%)$_{40}$-PEG(6k)$_{60}$	2.67	1230	34
7	Triol(1.5k, 35%)$_{60}$-PEG(6k)$_{40}$	2.85	680	71
8	Triol(2k, 35%)$_{60}$-PEG(6k)$_{40}$	2.81	610	68
9	Triol(4k, 35%)$_{60}$-PEG(6k)$_{40}$	2.69	1100	56

a: $\bar{f} = \frac{n_{Triol} \times 3 + n_{PEG} \times 2}{n_{Triol} + n_{PEG}}$

The individual scanning results of the precursors, Triol(2k, 50%), PEG(6k), and Triol(2k, 50%)-PEG(6k) networks with different Triol contents are shown in Figure 1, and the observable transition enthalpies and relevant temperatures of all samples are summarized in Table 3.

As is shown in Figure 1, the three networks (b-d) displayed obvious crystalline transition temperature, which was a prerequisite for shape-memory polymers, though the T_m of the networks shifted to the lower temperature compared to the pure PEG (6k) precursor (58°C). In addition, the T_m of the networks can be changed by the increment of the Triol content, and the crystalline enthalpy decreased from 51 j/g to 26.8 j/g, indicating that we could regulate the T_m of the networks by the interference of Triol content on the crystallization of PEG. Besides the T_m, the three networks (b-c) also showed recrystallization temperature (T_c) [18], which surprisingly increased with the enhancement of Triol content (–23°C, –15.5°C, –3.2°C, in turns), accompanying the recrystallization enthalpy, which decreased from 31 j/g to 23.4 j/g. In particular, network c displayed glass transition behavior, recrystallization, and crystal melting step by step in the range of temperature studied. However, the T_g (–28.3°C) of network c was lower than the pure Triol (–13°C), which may be due to the intermiscibility of the triol and PEG phase in the polyurethane network. Furthermore, the highest Triol content (60%, network c) resulted in the highest T_g value (–28.3°C) (entries 3–5, Table 3), since the T_g of the other two polyurethane networks was not detected in the testing range of DSC (–50°C) (entries

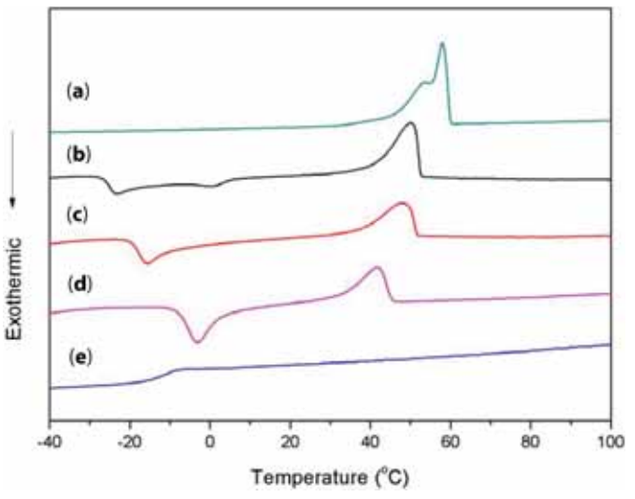

Figure 1 DSC curves of PEG(6k), Triol(2k, 50%) and Triol(2k, 50%)-PEG(6k) networks with different contents. a: PEG (6k), b: Triol(2k, 50%)$_{40}$-PEG(6k)$_{60}$, c: Triol(2k, 50%)$_{50}$-PEG(6k)$_{50}$, d: Triol(2k, 50%)$_{60}$-PEG(6k)$_{40}$, e: Triol(2k, 50%).

Table 3 Thermal characteristics of Triol-PEG networks from DSC analysis.[a]

		The third heating scan					
Entry	**Samples**	T_g (°C)	ΔC_p (j/g*°C)	T_c (°C)	ΔH_c (j/g)	T_m (°C)	ΔH_m (j/g)
1	Triol(2k, 50%)	-13	0.7	-	-	-	-
2	PEG(6k)	-	-	-	-	58	135.7
3	Triol(2k, 50%)$_{40}$-PEG(6k)$_{60}$	-	-	-23	–31	50.2	51
4	Triol(2k, 50%)$_{50}$-PEG(6k)$_{50}$	-	-	-15.5	-28.8	48	34.2
5	Triol(2k, 50%)$_{60}$-PEG(6k)$_{40}$	-28.3	0.7	-3.2	-23.4	42.4	26.8
6	Triol(2k, 20%)$_{40}$-PEG(6k)$_{60}$	-30.8	0.6	-	-	50.8	61.1
7	Triol(2k, 35%)$_{40}$-PEG(6k)$_{60}$	-	-	-26.9	-39.2	46.7	51.2
8	Triol(1.5k, 35%)$_{60}$-PEG(6k)$_{40}$	-	-	-3.8	-25.3	43.5	30.2
9	Triol(2k, 35%)$_{60}$-PEG(6k)$_{40}$	-	-	-3.1	-22.6	41.7	25.5
10	Triol(4k, 35%)$_{60}$-PEG(6k)$_{40}$	-	-	-3.5	-23.4	42.8	26.9

a: "–" indicates that the thermal behavior is not observed.

3-4, Table 3). Additionally, the T_c of the polyurethane increased with the increment of Triol content (entries 3–5, Table 3), which might further prove the intermiscibility of the Triol and PEG phase.

Figure 2 shows the DSC curves of Triol(2k)$_{40}$-PEG(6k)$_{60}$ networks produced from Triol(2k) precursor with different CU (20%, 35%, 50%). Network 'a' displayed glass transition temperature at –30.8°C, however, the networks 'b' and 'c' (CU = 35%, 50%, respectively) did not show glass transition, but recrystallization temperature, indicating that the CU of the triol might influence both the chain movement of the triol segment and PEG segment, since carbonate segment is more rigid than the ether segment in

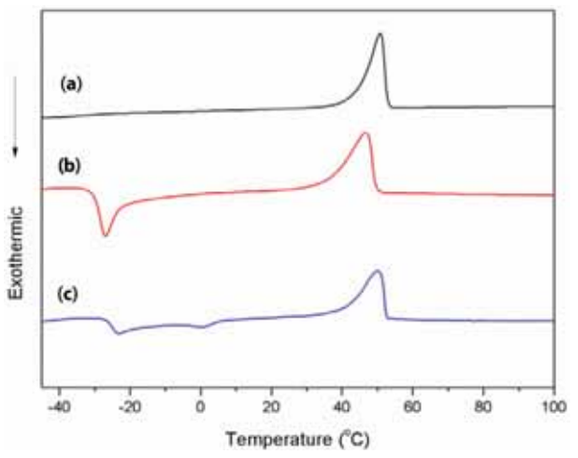

Figure 2 DSC curves of Triol(2k)$_{40}$-PEG(6k)$_{60}$ networks with different carbonate unit contents: (**a**) CU = 20%, (**b**) CU = 35%, (**c**) CU = 50%.

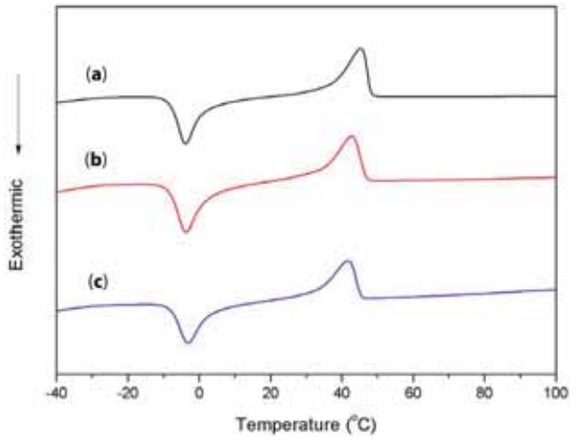

Figure 3 DSC curves of Triol(35%)$_{60}$-PEG(6k)$_{40}$ networks with different Triol M_ns: (**a**) 1500, (**b**) 2000, (**c**) 4000.

oligo(carbonate-ether) triol. The T_m of the network changed slightly with the variation of triol carbonate unit content, proving that the CU of the Triol could hardly influence the crystallinity of the PEG.

The effect of the M_n of the Triol precursors on the thermal behavior of Triol(35%)$_{60}$-PEG(6k)$_{40}$ networks is presented in Figure 3. The M_n of the Triol had almost no effect on the thermal behavior of the Triol-PEG networks in this experimental condition, since the T_m (~ 42°C) and T_c (~ –3.5°C) did not change obviously when M_n of the Triol increased from 1500 g mol^{-1} to 4000 g mol^{-1}, which was the same as in the previous reports [12]. In addition, as can be seen from Table 3, recrystallization temperature and recrystallization enthalpy also did not obviously change with the variation of the M_n of the Triol. However, the gel content of the networks decreased from 71% to 56%, indicating that the crystallization of the networks was not influenced by gel content.

3.4 Shape-Memory Effect of Triol-PEG Networks

It is well-known that there is always a microphase separation in segmented polyurethanes, that is, a hard phase and soft phase appear [23]. However, in the crosslinked PU, it is difficult to distinguish the two phases above. Compared to common polyurethanes, amorphous Triol could afford networks with crosslinking structure and, what's more, the amorphous segments could store more elastic energy to recover its original shape. Besides, PEG gave networks a considerable crystallinity. It is that specialty that leads to the shape-memory property of the networks. The important quantities to be determined for describing shape-memory properties of a material are the shape fixity ratio (R_f) and the shape recovery ratio (R_r). Shape fixity ratio qualifies the ability of the material to memorize its permanent shape, whereas shape recovery ratio describes the ability of the switching segment to fix the mechanical deformation. For a dual-shape system, the covalent crosslinks of the Triol served as netpoints which determined the permanent shape, while the crystalline PEG chains served as molecular switch segments (T_{trans} = T_m), fixing the temporary shape at temperature below T_{trans}. Therefore, increasing the content of PEG could improve the shape-memory effect of network under sufficient crosslinking.

Figure 4 describes the effect of the composition of the precursors on the shape-memory effect of the networks. The R_f decreased from 100% to 65% with an increase of the Triol content (from 40% to 60%). Surprisingly, R_r did not change obviously (all nearly 100%). The high crystalline PEG content could afford network with high crystallization domain and thus well shape fixity ratio. However, increasing the Triol content resulted in the increase of the crosslink density and the decrease of PEG content, both of which were detrimental to the crystallity of PEG, so R_f decreased with increasing the Triol content. The flexible amorphous Triol could store more elastic energy than the rigid crystalline ones, so that the networks changed from a rigid plastic to soft rubber with the increase of the Triol content. What's more, deformation at high temperature (70°C, approximately 20°C above T_m) was

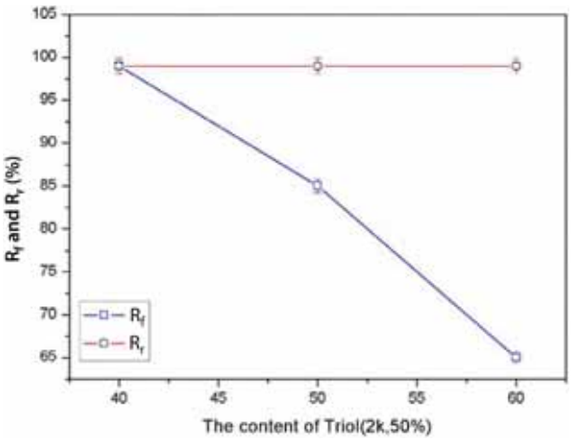

Figure 4 The shape-memory effect of Triol(2k)-PEG(6k) networks with different Triol(2k, 50%) content.

much easier due to the lower rubbery modulus of the polymer that made the orientation of polymer more feasible. It was for these reasons that all the R_r of the networks reached nearly 100%. The CU of the Triol had no influence on the shape-memory effect of the network, since R_f and R_r did not change obviously.

The shape recovery rate is another important factor to evaluate the shape-memory performance of the networks. The effect of the Triol(2k, 50%) content (a) and the Triol(2k) CU (b) on the recovery time is shown in Figure 5. Increasing the Triol content (from 40% to 60%) resulted in much faster recovery (from 62 s to 40 s), due to the increase of crosslink density (a). Interestingly, increasing the substructure of the Triol CU, led to the alteration of the recovery time, which might be attributed to the greater rigidity of the carbonate segment than ether segment in the oligo(carbonate-ether) triol. Therefore, apart from the traditional method (changing the precursors content), in the present work, we could regulate the recovery time of the networks simply by pre-designing the CU of the Triol. In addition, the numbers of shape-memory testing had no influence on R_f and R_r, suggesting that the networks could keep the dual-shape effect well. For a more direct observation of the shape-memory effect of the Triol-PEG networks, the macroscopic behavior of these materials is demonstrated in Figure 6. A strip-type sample of Triol(2k, $50\%)_{40}$-$PEG(6k)_{60}$ was changed into a bending shape at 70°C and then cooled rapidly to room temperature, and it returned to the original shape in about 1 min at 70°C. Interestingly, the deformed sample almost immediately recovered its original shape (in less than 3 s) when immersed in 70°C water. There are possibly two roles that water plays in the interaction with triol-PEG networks. Firstly, water dissipates into the polymeric matrix that affects their microstructure, the regular

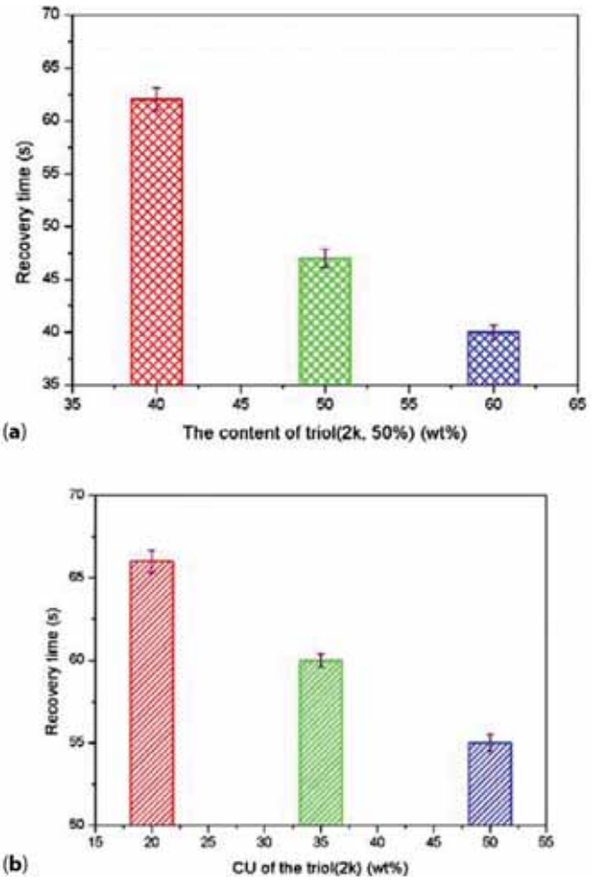

Figure 5 The effect of the content of Triol(2k, 50%) (**a**) and the CU of the Triol(2k) (**b**) on the recovery time.

arrangement of the molecular chains is disturbed and the molecular chains are easier to move, therefore, the networks can recover their original shape. Secondly, since the heat transfer coefficient of water is superior to air, the PEG part in the Triol-PEG network melts more quickly in 70°C water than in 70°C air. Thus, the shape-memory effect is driven by crosslinks within the system via entropic elasticity. The excellent shape recovery of triol-PEG networks in water indicates that the recovery stress is large enough for some application within a constraint environment.

3.5 Mechanical Properties of Triol-PEG Networks

The mechanical properties measurement allowed us to further acknowledge the performance of Triol-PEG networks. Figure 7 displays the mechanical properties

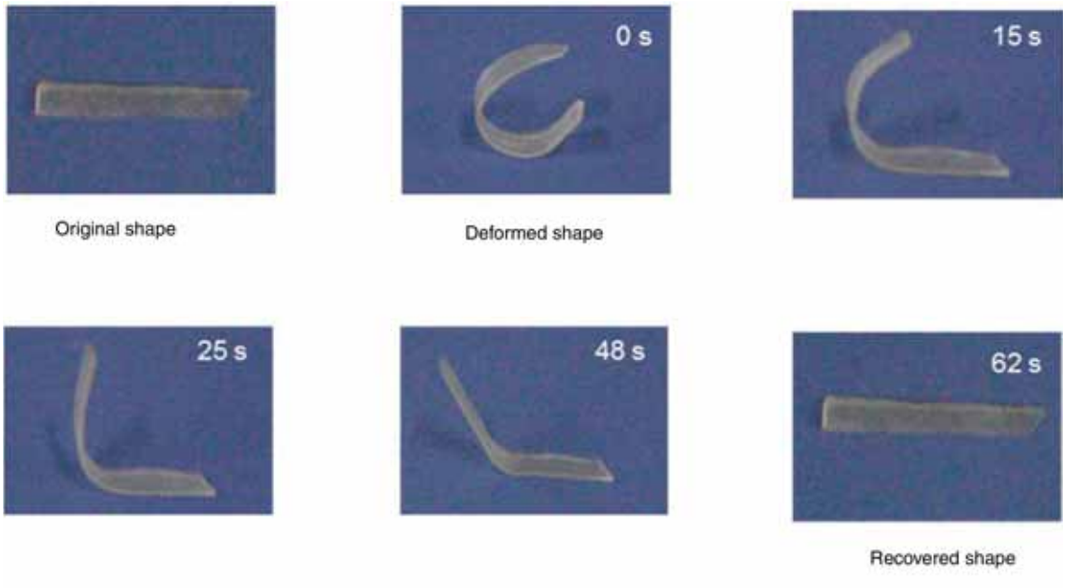

Figure 6 Recovery process of a strip-shaped sample of Triol(2k, 50%)$_{40}$-PEG(6k)$_{60}$ at 70°C.

(tensile strength σ, elongation at break ε) of different Triol-PEG networks with different Triol(2k, 50%) content (a), different CU of the Triol (b), different M_n of the Triol (c). For networks prepared with different Triol(2k, 50%) content (a), both σ and ε increased with an increase of the Triol content. This might be ascribed to the tensile strength of networks which increased with the increase of the crosslink density. Besides, Triol as the macromolecular crosslinking agent could reduce the crosslink density of the network (< 80%), resulting in the increase of ε with the increase of Triol content. A typical sample Triol(2k, 50%)$_{60}$-PEG(6k)$_{40}$ showed good mechanical performance with a σ of 5.5 MPa and ε of 560%. For networks prepared with different CU of the Triol (b), σ increased with the enhancement of the CU of the Triol, whereas, ε showed a slight variation, indicating that the chain rigidity (increase of Triol CU of (b)) may improve the σ signifcantly. For networks prepared with different M_n of the Triol (c), when the M_n of the Triol was 2000 g mol^{-1}, the network displayed the highest ε and the lowest σ among 1.5k–4k Triol molecular weights.

3.5.1 Cytotoxicity of Triol(2k, 50%)$_{60}$-PEG(6k)$_{40}$ network

Since PEG has excellent biocompatibility, the present work has focused on the networks with higher Triol content, such as Triol(2k, 50%)$_{60}$-PEG(6k)$_{40}$ network, to identify its cytotoxicity. The cells grew well after being incubated in culture medium containing different weight samples for 24 h (Figure S2); for the quantitive observation of cell viability, MTT essay was taken, as shown in Figure 8.

4 CONCLUSIONS

The bulk CO_2-based Triol was successfully applied in shape-memory polyurethanes, which might promote the further development of SMPs. The resulting Triol-PEG networks displayed good dual-shape effect: shape fixity ratio (R_f) could be controlled by changing the Triol content, all the shape recovery ratio (R_r) of the network could approach 100% under the experimental conditions; in particular, the substructure, the CU of the Triol had a significant effect on the recovery time of the networks. The amorphous structure of Triol contributed to high elastic energy, which could recover its original shape in less than 3 s (70°C water). The good biocompatibility might afford network with biomedical application.

ACKNOWLEDGMENTS

The authors thank the National Natural Science Foundation of China (grant no. 51321062, 51273197 and 21134002) for financial support.

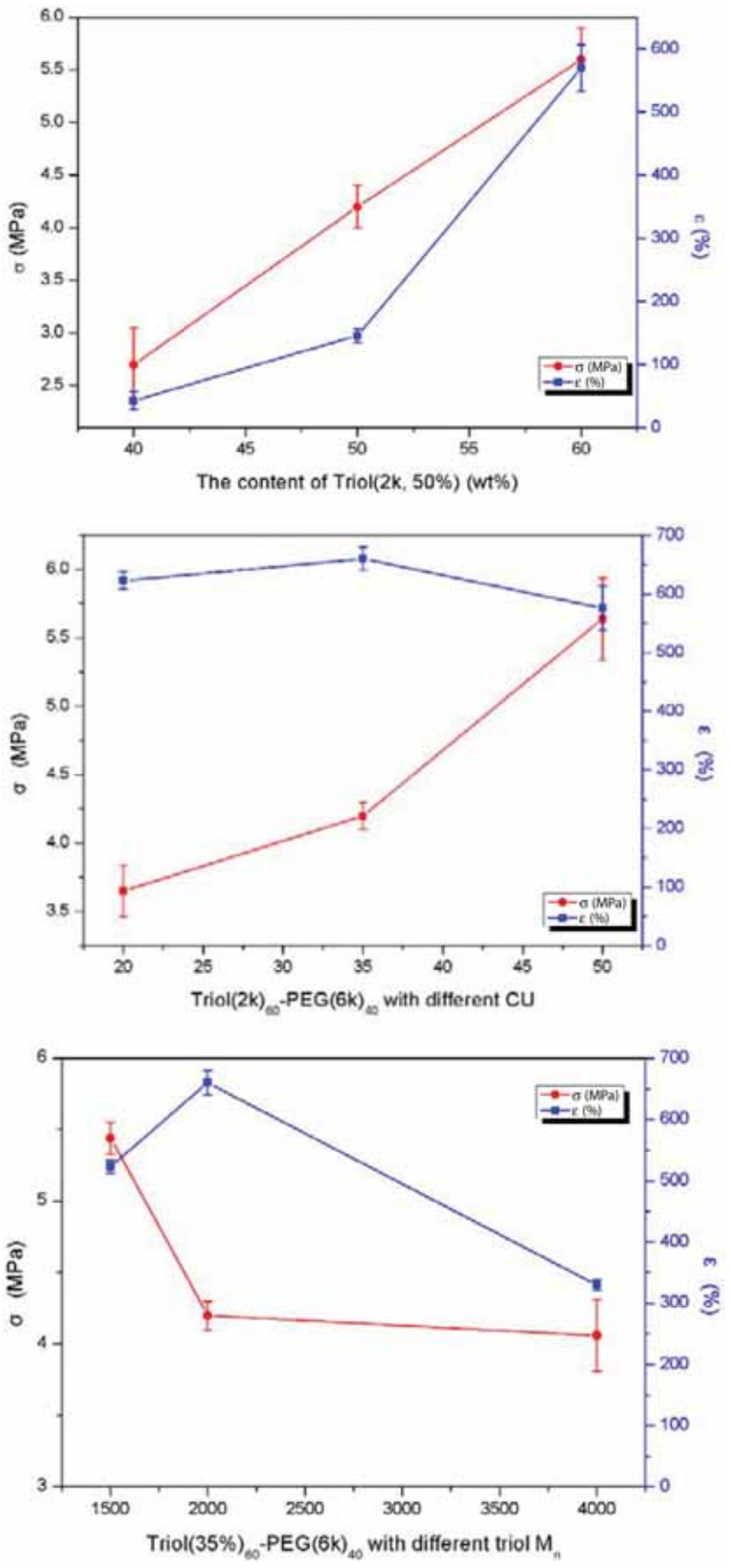

Figure 7 Mechanical performance of Triol-PEG(6k) networks: (**a**) Triol(2k, 50%)-PEG(6k); (**b**) $Triol(2k)_{60}$-$PEG(6k)_{40}$; (**c**) $Triol(35\%)_{60}$-$PEG(6k)_{40}$.

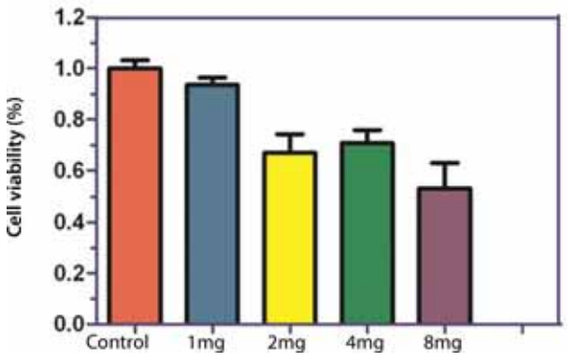

Figure 8 Proliferation of Hela cells on Triol(2k, $50\%)_{60}$-PEG(6k)$_{40}$ network film with different weights (MTT assay results).

REFERENCES

1. P. Ping, W. Wang, X. Chen, and X. Jing, Poly (ε-caprolactone) polyurethane and its shape-memory property.*Biomacromolecules* **6**, 587–592 (2005).
2. B. K. Kim, S. Y. Lee, and M. Xu, Polyurethanes having shape memory effects. *Polymer* **37**, 5781–5793 (1996).
3. J. Hu, Y. Zhu, H. Huang, and J. Lu, Recent advances in shape–memory polymers: Structure, mechanism, functionality, modeling and applications. *Prog. Polym. Sci.* **37**, 1720–1763 (2012).
4. A. Lendlein and S. Kelch, Shape-memory polymers. *Angew. Chemie Intl Ed.* **41**, 2034–2057 (2002).
5. Y. Shao, C. Lavigueur, and X. X. Zhu, Multishape memory effect of norbornene-based copolymers with cholic acid pendant groups. *Macromolecules* **45**, 1924–1930 (2012).
6. A. Lendlein, H. Jiang, O. Junger, and R. Langer, Light-induced shape-memory polymers. *Nature* **434**, 879–882 (2005).
7. J. R. Kumpfer and S. J. Rowan, Thermo-, photo-, and chemo-responsive shape-memory properties from photo-cross-linked metallo-supramolecular polymers. *J. Am. Chem. Soc.* **133**, 12866–12874 (2011).
8. R. Mohr, K. Kratz, T. Weigel, M. Lucka Gabor, M. Moneke, and A. Lendlein, Initiation of shape-memory effect by inductive heating of magnetic nanoparticles in thermoplastic polymers. *Proc. Natl Acad. Sci. USA* **103**, 3540–3545 (2006).
9. A. Metcalfe, A. C. Desfaits, I. Salazkin, L. H. Yahia, W.M. Sokolowski, and J. Raymond, Cold hibernated elastic memory foams for endovascular interventions. *Biomaterials*, **24**, 491–497 (2003).
10. W. Small Iv, T. Wilson, W. Benett, J. Loge, and D. Maitland, Laser-activated shape memory polymer intravascular thrombectomy device. *Opt. Expr.* **13**, 8204–8213 (2005).
11. H. Tobushi, H. Hara, E. Yamada and S. Hayashi, Thermomechanical properties in a thin film of shape memory polymer of polyurethane series. *Smart Mater. Struct.* **5**, 483–491 (1996).
12. Y. Niu, P. Zhang, J. Zhang, L. Xiao, K. Yang, and Y. Wang, Poly (p-dioxanone)–poly (ethylene glycol) network: synthesis, characterization, and its shape memory effect. *Polym. Chem.* **3**, 2508–2516 (2012).
13. D. Ratna and J. Karger Kocsis, Recent advances in shape memory polymers and composites: a review. *J. Mater. Sci.* **43**, 254–269 (2008).
14. C. M. Yakacki, R. Shandas, D. Safranski, A. M. Ortega, K. Sassaman, and K. Gall, Strong, tailored, biocompatible shape-memory polymer networks. *Adv. Funct. Mater.* **18**, 2428–2435 (2008).
15. J. Li and T. Xie, Significant impact of thermo-mechanical conditions on polymer triple-shape memory effect. *Macromolecules* **44**, 175–180 (2010).
16. J. H. Yang, B. C. Chun, Y. C. Chung, and J. H. Cho, Comparison of thermal/mechanical properties and shape memory effect of polyurethane block-copolymers with planar or bent shape of hard segment. *Polymer* **44**, 3251–3258 (2003).
17. W. Wang, P. Ping, X. Chen, and X. Jing, Polylactide-based polyurethane and its shape-memory behavior. *Eur. Polym. J.* **42**, 1240–1249 (2006).
18. J. Lin and L. Chen, Study on shape-memory behavior of polyether-based polyurethanes. I. Influence of the hard-segment content. *J. Appl. Polym. Sci.* **69**, 1563–1574 (1998).
19. B. K. Kim, S. Y. Lee, J. S. Lee, S. H. Baek, Y. J. Choi, J. O. Lee, and M. Xu, Polyurethane ionomers having shape memory effects. *Polymer,* **39**, 2803–2808 (1998).
20. H. M. Jeong, J. B. Lee, S. Y. Lee, and B. K. Kim, Shape memory polyurethane containing mesogenic moiety. *J. Mater. Sci.* **35**, 279–283 (2000).
21. J. R. Lin and L. W. Chen, Shape-memorized crosslinked ester-type polyurethane and its mechanical viscoelastic model.*J. Appl. Polym. Sci.* **73**, 1305–1319 (1999).
22. A. Alteheld, Y. Feng, S. Kelch, and A. Lendlein, Biodegradable, amorphous copolyester-urethane networks having shape-memory properties. *Ang. Chem. Int. Ed.* **44**, 1188–1192 (2005).
23. J. Xu, W. Shi, and W. Pang, Synthesis and shape memory effects of Si–O–Si cross-linked hybrid polyurethanes. *Polymer* **47**, 457–465 (2006).
24. L. P. Xiao, M. Wei, M. Q. Zhan, J. J. Zhang, X. Y. Deng, K. K. Yang, and Y. Z. Wang, Novel triple-shape PCU/PPDO interpenetrating polymer networks constructed by self-complementary quadruple hydrogen bonding and covalent bonding. *Polym. Chem.* **5**, 2231–2241 (2014).
25. M. Bonfil, A. Sirkecioglu, O. Bingol Ozakpinar, F. Uras, and F. S. Güner, Castor oil and PEG-based shape memory polyurethane films for biomedical applications. *J. Appl. Polym. Sci.* **131** (2014).
26. S. Liu, Y. Qin, X. Chen, X. Wang, and F. Wang, One-pot controllable synthesis of oligo (carbonate-ether) triol using a Zn-Co-DMC catalyst: the special role of trimesic acid as an initiation-transfer agent. *Polym. Chem.* **5**, 6171–6179 (2014).

Supplementary materials:

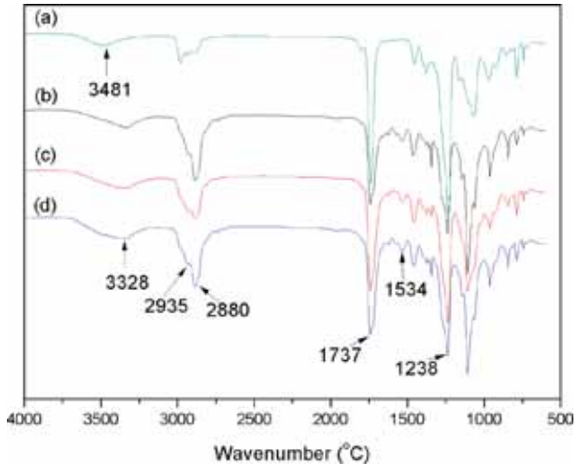

Figure S1 ATR FT-IR spectra of (a) Triol(2k, 50%), (b) Triol(2k, 50%)$_{40}$-PEG(6k)$_{60}$, (c) Triol(2k, 50%)$_{50}$-PEG(6k)$_{50}$, (d) Triol(2k, 50%)$_{60}$-PEG(6k)$_{40}$.

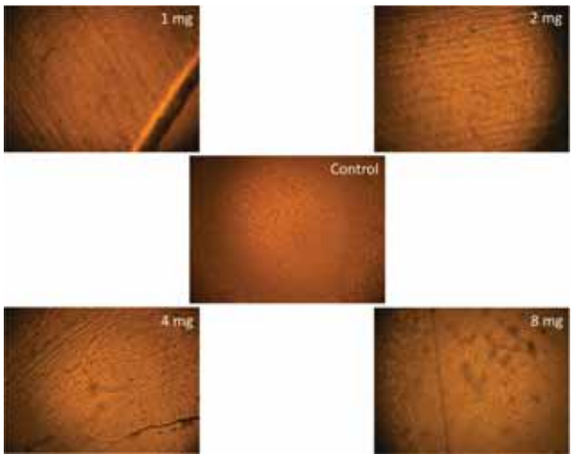

Figure S2 The direct contact test of Hela cells with different weight content of Triol (2k, 50%)$_{60}$-PEG(6k)$_{40}$ networks as displayed in the picture; wells containing cells but no polymer were used as control.